JPIChE 52 (2) 2024: 69-77

PAKISTAN INSTITUTE OF CHEMICAL ENGINEERS Since 1969

Journal of the Pakistan Institute of Chemical Engineers

Journal homepage: www.piche.org.pk/journals

DOI: https://doi.org/10.54693/piche.05228

Check for updates

Silver Doped CeO_2 Nanocomposites for Photo Degradation of Selected Azo Dyes

M. Hussain[1], G. Ali[2], F. Hussain[3], M. Hussain[4], M. M. Arif[5]*

Submitted: 20/11/2024, Accepted: 15/04/2025, Published: 22/04/2025

Abstract

The sol-gel approach was employed to synthesize silver-doped CeO_2 nanoparticles exhibiting superior photocatalytic activity under solar light irradiation. The produced catalysts were characterized using techniques such as Fourier transform infrared spectrophotometry (FTIR), X-ray powder diffraction (XRD), scanning electron microscopy (SEM), energy dispersive X-ray spectroscopy (EDX), Dynamic light scattering (DLS) and UV-vis spectrometry. These approaches were also useful for analyzing the absorption spectra and the concentration of azo dyes in water at variance concentrations of during the photodegradation experiment. Research results indicated that anatase phase nanoparticles of pure CeO_2 and silver (Ag) doped CeO_2 have crystallite sizes that range between 15 and 18 nm. It was found that Ag/ CeO_2 catalyst enhances the performance and light absorption capabilities of nanoparticles as compared to pure CeO_2. Ag/CeO_2 nanoparticles are an attractive option for photocatalytic purification of other organic-based wastewater exposed to sunlight because of their significant photocatalytic efficacy in visible light, deep catalytic constancy, and reusability for dye photocatalysis.

Keywords: Photocatalytic Degradation, Azo Dyes, Ag/CeO_2 Nano Powders, Sole-gel

1. Introduction:

One of the main worldwide issues of this era is to address the energy disaster and reduce pollution using affordable and simple methods. A large quantity of wastewater from textile and other sectors consists of various harmful pollutants including organic contaminants and synthetic colors. Typically, this wastewater is released into aquatic bodies without sufficient treatment [1]. Development of dye removal from wastewater is more important than other colorless organic contaminants in preventing environmental pollution because it has a greater impact on the aquatic ecosystem [2]. Thus, it is worthwhile to design an effective and environmentally acceptable technology that uses the full sun spectrum to solve water contamination concerns. Photocatalysis with sunlight exposure is an efficient, cost-effective, and extensively utilized technique.

Photocatalysis is one of the most interesting uses of solar energy. Photocatalysis is a material that uses the synergetic action of catalysts and light for the energy conversion process. Photocatalysis is a novel category of green technology that uses a high-speed process to destroy pollutants (especially specific azo dyes) and obtain the most hydrogen energy from water and sunlight. The use of electrons and holes is the most

[1] *Department of Environmental Engineering, University of Chinese Academy of Sciences, China*
[2] *Department of Software Engineering, University of Okara, Okara, Pakistan*
[3] *Department of Mathematics, Virtual University of Pakistan, Pakistan*
[4] *Department of Mathematics (Division of Science and Technology), University of Education, Lahore, Pakistan*
[5] *Virtual Lab Private Limited, Lahore, Pakistan*

*** Corresponding author:** M. Maaz Arif (maazarifbutt@gmail.com)

intriguing component of Photocatalysis. The production of charge carriers (electrons and holes) starts the Photocatalytic processes that are stimulated by light and perfect Photocatalysts always should have a huge photo absorption range and good photo-generated charge carrier separation efficiency [3].

Photocatalysis is thought to be an efficient method for reducing pollution in the environment. To cope with these possible dangers, photocatalysis utilizing semiconductor composites has been employed. Many photocatalysts have been evaluated for their ability to remove chemical pollutants and hazardous gases, among other things. Ceria has been regarded as a promising photocatalytic material, influence of size and shape on its activities has been studied. When compared to micro sized grains, the electronic conductivity of nano sized ceria is extremely high. Ceria absorbs visible light and it has been demonstrated that combining it with Titania promotes effective charge separation. As a result, photocatalysis under visible light may be achieved using ceria or based composites produced utilizing the selective method [4].

CeO_2 is one of the most studied photocatalysts due to this catalyst's excellent optical and thermal properties, chemical stability, less toxicity, low cost, high photoactive, reusability and eco friendliness [5-7]. Due to its substantial band gap of 3.2 eV, CeO_2 may be triggered by UV light with wavelengths less than 387 nm. However, the solar spectrum contains approximately 4% UV light, so the optical response of CeO_2 to the visible light region will increase the photocatalytic activity of this catalyst. Consequently, efforts to make CeO_2 incorporate visible light deserve high attention from the perspective of using solar light energy with greater effectiveness [8].

Numerous researchers have examined various approaches to attain this objective, one of which involves the utilization of composite metal oxides synthesized by doping CeO_2 with transition metal oxides such as Ag, Mn, C, and Fe. These oxides have the ability to absorb the visible light by reducing their band gap [8-11]. CeO_2 nano particles have a high band gap (3.2 eV) which means that they can only be triggered by UV radiation, which is one of their key disadvantages. CeO_2 has a high electron-hole recombination rate which significantly reduces photocatalytic performance, is another significant drawback.

Silver ions have gained the interest of various researchers in current centuries, remaining both for their new effects on the enhancement of photo activity of semiconductor photo catalysis nano-crystallites and their antibacterial activity. Silver (Ag) doped CeO_2 was synthesized through homogeneous precipitation mixed with a homogeneous/impregnation technique under visible light, in which 1.5 percent mole of Ag-doped CeO_2 demonstrated the greatest percentage removal. It was found that for dye treatment CeO_2 modified by doping with silver makes the catalyst more effective and shortens the illumination duration [12].

Notwithstanding its widespread recognition, the sol-gel approach is incredibly easy to use and doesn't call for any specialized tools to create ceria nanoparticles. Thermal stability and photocatalytic activity are enhanced by the tiny crystalline size and excellent crystalline phase of CeO_2 produced using this approach [13].

In this work, we produced silver doped CeO2 nanoparticles using the sol-gel process at various silver concentrations. The photocatalytic activity of the produced samples was determined by the degradation of methylene blue, methyl red, methyl orange, and malachite green in aqueous solution under solar light irradiation.

The objective of this work is to prepare nano-scaled CeO_2 nanoparticles, effectively dope them with silver, characterize and assess the photocatalytic performances of these materials under sunlight.

2. Materials and Methods:

2.1. Materials:

Cerium nitrate hexahydrate ($Ce(NO_3)_3.6H_2O$), Ammonium hydroxide (NH_4OH) or Sodium hydroxide (NaOH), Urea (CH_4N_2O), Hydrochloric acid (HCL), methylene blue, methyl orange, methyl red, malachite green and distilled water. All the reagent-grade and chemicals were used without further purification.

2.2. Preparation of Aqueous CeO_2 nano sol and CeO_2 Nano Powder:

For the manufacture of CeO_2 powder, the sol-gel technique was utilized. A straight sol-gel approach was utilized to create cerium NPs from cerium oxide. For synthesis of nanoparticles effective parameters were optimized [14]. Firstly, precursor ($Ce(NO_3)_3.6H_2O$) was mixed in distilled water, maintaining pH 10 by the addition of ammonium hydroxide or sodium hydroxide

and further stirred it for 2 h. Secondly, a urea solution of defined concentration was prepared at constant pH 2 by the addition of HCL.

After preparing the solution, we mixed both solutions by adding urea solution dropwise and then stirring for two hours. After that, get ceria nano-sol. Prepared nano-sol stored in a refrigerator at 4^{o}C [15]. After preparing ceria nano-sol, put the ceria sol into the oven for 35 to 40 hours at a 70-85^{o}C temperature. Then calcined it for 2 h, at a 600^{o}C temperature in the furnace and ceria crystals formed. Then added 2 mg ceria in 10 ml dyes (methyl blue, methyl red, methyl orange and malachite green) at different pH (3, 7 and 11) to check the activity of material after place it under sun light for 1 h.

2.3. Characterizations of Synthesized System:

Prior to examining the photocatalytic performance of prepared pure CeO_2 and Ag/CeO_2 catalysts, these were examined for crystal structure and particle size using X-ray diffraction (XRD) with a Shimadzu X-ray diffractometer. Using the SHIMADZU IRTracer-100, Fourier transform infrared spectroscopy (FTIR) is used to assess and clarify optical characteristics and structural features. Using JEOL JSM-7000F equipment, scanning electron microscopy (SEM) and energy-dispersive X-ray spectroscopy (EDX) were utilized to examine the sample's surface morphology and elemental composition. With the use of an ultraviolet visible spectrophotometer (Hitachi U-2001 beam spectrophotometer), the light absorption spectra of the sample were determined.

The degradation of azo dyes (methylene blue, methyl red, methyl orange, and malachite green) in an aqueous solution at room temperature was used to assess the photocatalyst activities of the produced sample. Each experiment involved adding 0.1 g of photocatalyst to a Pyrex glass beaker holding the solution of dyes, almost 100 ml with a starting concentration of 0.02 mg/100 ml of water. To create adsorption-desorption equilibrium, each suspension was magnetically agitated for 30 minutes in the dark before being exposed to sun radiation. Next, the mixture was stirred and exposed to sunshine. A Hitachi U-2001 UV-vis spectrophotometer was used to measure the dye concentration every 30 minutes during irradiation by measuring the absorbance at 510 nm.

Dye's degradation rate was calculated with the help of this formula:

Degradation percentage = $[(C_0 - C) / C] \times 100$

Where C is the concentration at each time interval in milliliters L-1 and C_0 is the initial concentration of all dyes in milliliters L-1.

3. Results:

3.1. XRD:

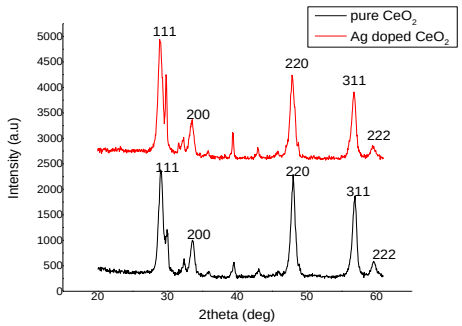

Figure 1: XRD spectra of synthesized silver doped CeO_2 NPs. Here are signifies relates to Ag and CeO_2 characteristic diffraction peaks

The XRD patterns of pure cerium oxide and silver decorated CeO_2 nanoparticles are shown in Fig. 1. The distinct cubic structure of CeO_2 with its distinctive plane of (1 1 1) orientation is evident in the pure nanoparticles. The outcome that was obtained matches the standard data quite well. Crystalline silver peaks are formed along CeO_2 peaks with the main characteristic of silver (1 1 1) plane in the case of Ag integrated CeO_2 nanoparticles. The obtained Ag peaks match the cubic structure of silver quite well. Furthermore, the mixture of silver does not show any noticeable peak shifts in the CeO_2 pattern showing the silver is present on the surface rather than in the spaces between particles or gap regions of CeO_2. The average crystallite size of pure CeO_2 nanoparticles is calculated to be 19.27 nm, whereas the size of the Ag-incorporated CeO_2 nanoparticles dropped to 18.2183 nm.

The reduction in crystallite size is evidently visible in the peak expansion depicted in Figure 1. Aside from that, the size of silver (Ag) crystallites was determined to be 19.27 nm. Resulting major silver peaks are shown to be evenly distributed over the CeO_2 surface. Furthermore, as-synthesized CeO_2 nanoparticles have a somewhat higher lattice parameter (~5.414 Å) than bulk CeO_2 (~5.411 Å). Ag-doped samples show a larger CeO_2 lattice parameter (~5.553 Å), possibly due to increased surface defects and smaller crystallite size.

Table 1: Crystallite size calculation of Ag doped CeO_2

2 θ (deg)	(hkl)	FWHM	Crystal size (nm)	d-spacing(Å)
28.70	(111)	0.4385	19.53	3.1233
33.23	(200)	0.3635	23.81	2.7049
47.64	(220)	0.5814	15.59	1.9126
56.47	(311)	0.6217	15.14	1.6311
59.24	(222)	0.9625	9.91	1.5617
Average crystallite size			18.2183	

3.2. FTIR:

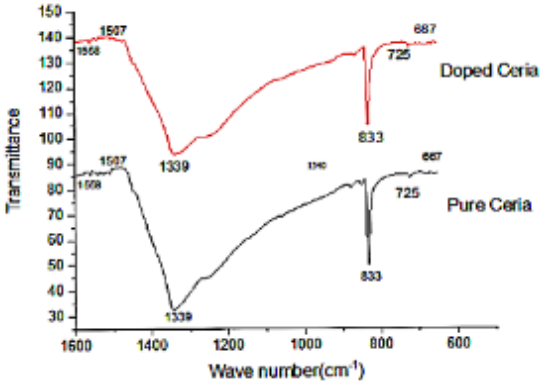

Figure 2: FT-IR of Pure CeO_2, Ag doped CeO_2 with table of peaks

Table 2: Peaks of FT-IR (cm^{-1})

Peaks(cm^{-1})	Assignments
667	Ce-O bond
725	Ce-O bond
833	Metal-O bond
1339	CH_2 bond
1507	CH_2 bond
1558	Water bonding

The FTIR scales used to analyze the adsorption classes on surfaces of produced CeO_2 and silver coated CeO_2 NPs are shown in Figures 2. The range of FT-IR spectrum of pure CeO_2 was 600 to 1600 cm^{-1}. This spectrum showed five absorbance peaks at 667, 725, 833, 1339, 1507 and 15cm^{-1}. The distortion approach of the Ce-O bond is liable for the main absorption group detected at 667 cm^{-1}. Additional peaks observed at 1595 cm^{-1} relate to O-H twisting atmospheres and the peak at 2109 cm^{-1} corresponds to Ce-O extending ambiances. The Ag decorated CeO_2 samples clearly exhibit an extra top at 833 cm^{-1} that might be attributable to the creation of Ag-O extending feelings. The peak at 1558 cm^{-1} is due to symmetric bending of H_2O, whereas the peak around 1507 cm^{-1} reveals the extending sensations of CH_2 bonding adsorbed from ambient.

3.3. SEM and X – Ray Spectroscopy:

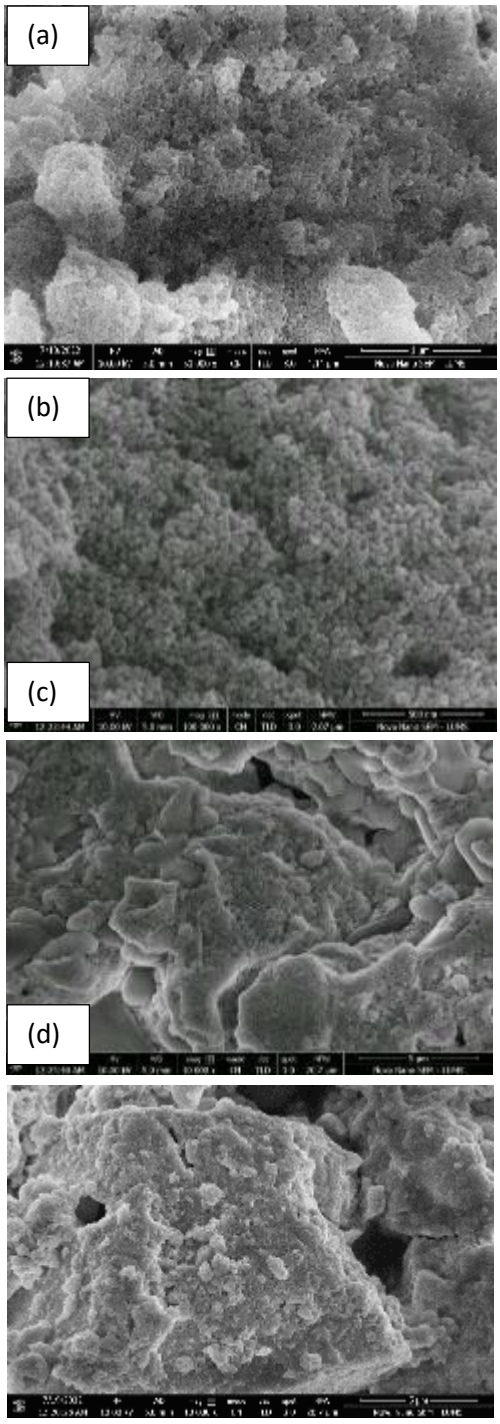

Figure 3: Morphological analysis of (a, b) pure CeO_2 and (c, d) silver doped CeO_2 NPs

The microstructural properties of pure CeO_2 and silver doped CeO_2 NPs are studied by SEM at various amplifications and findings are shown in Fig. 3. It is

evident that resulting particle sizes are clearly in nano scale series with accumulation. Furthermore, pure CeO_2 nanoparticles have a spherical form but Ag coated nanoparticles have cumulative size and definite grain limitations (Fig. 3. c, d). This nanostructure finding suggests that crystalline silver strength is bounded by CeO_2 particles. Fig. 3(c–d) indicate the various amplification pictures of silver doped nanoparticles, it showed uniform shape and size with regular distribution. It is clear from the higher magnification results that crystallite with sizes ranging from 8 to 20 nm are present. It is obvious from the higher magnification data that there are crystallites ranging in size from 8 to 20 nm.

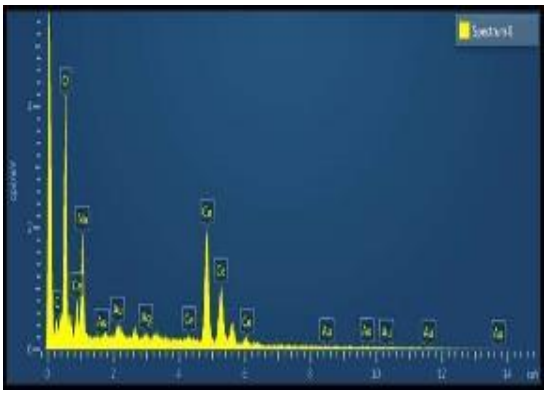

Figure 4: EDX spectrum with different elements and weights

Table 3: The Ag/CeO_2 NPs express an optical absorption band peak. EDX results confirm the development of Ag doped CeO_2 nanoparticles.

Element	Line Type	Apparent Concentration	k Ratio	Wt%	Wt% Sigma	Standard Label	Factory Standard
C	K series	0.49	0.00494	2.31	0.75	C Vit	Yes
O	K series	25.89	0.08712	25.64	0.62	SiO_2	Yes
Na	K series	5.08	0.02145	10.55	0.4	Albite	Yes
Ag	L series	0.72	0.0072	1.52	0.43	Ag	Yes
Ceria	L series	29.51	0.27467	57.64	0.9	CeO_2	Yes
Au	M series	0.9	0.00902	2.35	0.55	Au	Yes
Total:				100			

Silver salt doped cerium oxide shows the other contaminations and other impurities weights as C, O, Na, Ag, Ceria, and Au with different weights and show the presence of Silver in cerium oxide.

3.4. DLS (Dynamic light scattering):

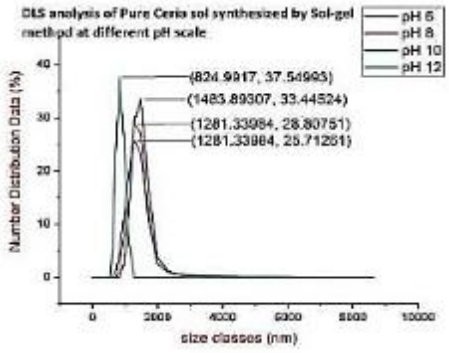

Figure 5: Dynamic light scattering at different pH

It showed about the particle size of catalyst and the effect of pH on it, as pH increased the size of particle decreased. The size of particle not in nano scale due to its coagulation and particles are in large size because particles are merged to each other.

3.5. UV-Visible Spectroscopy:

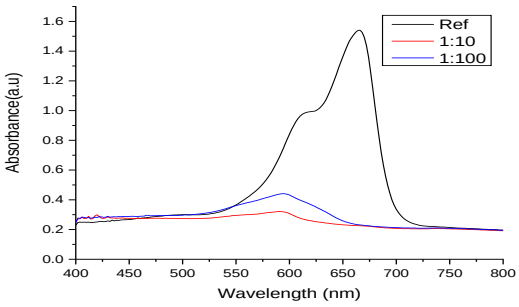

Figure 6.a: Methylene blue dye

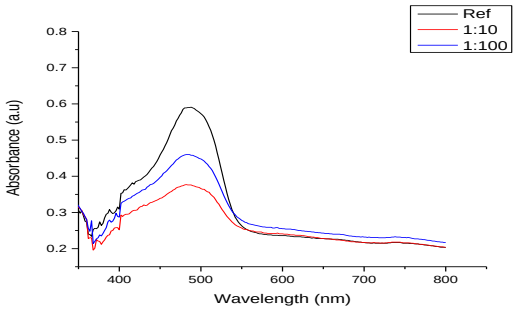

Figure 6.b: Methyl red dye

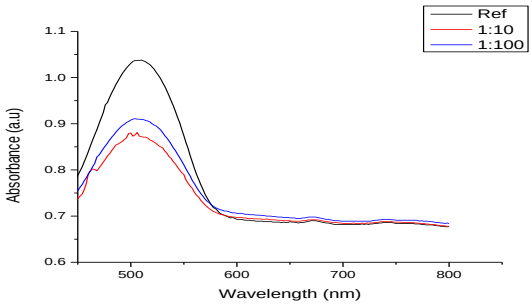

Figure 6.c: Methyl orange dye

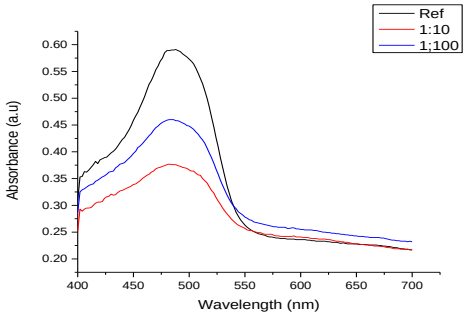

Figure 6.d: Malachite green dye

Fig. 6. depicts the UV-visible spectra of dyes and each dye contains the same ratios such as 1:10, 1:100 and pure CeO_2.It is noted that the dye solution with pH 11 shows the best results as compared to others. Figure 6.a depicts the UV-Visible spectra of methylene blue dye degradation employing an Ag doped CeO_2 catalyst with a 20-minute irradiation time interval under sunlight. Fig. 6.b depicts UV-Visible spectra of methyl red dye degradation employing an Ag doped CeO_2 catalyst with a 180-minute irradiation time interval under sunlight. The UV-Visible spectra of methyl orange dye degradation utilizing an Ag - CeO_2 catalyst with irradiation are shown in Figure 6.c. Figure 6.d depicts the UV-Visible spectra of malachite green dye degradation employing an Ag doped CeO_2 catalyst with a 15-minute irradiation interval under sunlight. The symmetric bending of H_2O causes the peak around 1600 cm^{-1}, but the stretching vibrations of CO absorbed from ambient CO_2 cause the peak at 2350 cm^{-1}. The extending vibration of the OH group created a modest peak about 3400 cm^{-1} over a 180-minute time span under sunlight. The absorption of dye molecules steadily decreases with increasing irradiation duration of degradation owing to chromosphere depletion to generate a transitional product. Degradation percent = $((C_O-C_t)/C_O)$ 100, is used to determine the degradation efficiency of the catalyst. Where C_t is the absorbance of the solution at a forementioned time, and C_o is the absorbance of the dye solution initially. The photocatalytic process was optimized and dyes degraded at pH 11 in direct sunlight exposure.

Discussion:

The X-ray diffraction (XRD) examination of Ag-doped CeO2 nanoparticles was conducted utilizing an analytical X'pert PRO model X-ray powder diffractometer and Cu-Kα radiation. Nanoparticles have been coated onto a glass substrate for XRD work. Average particle size was calculated by the d-Sherrer formula as a result of full width at half maximum (FWHM) data. The equation is presented such as:

$D = (k \lambda)/(\beta \cos \theta)$

where D signifies the crystal size in nanometers (nm), k represents the Sherrer constant valued at 0.94, λ denotes the wavelength at 0.15406 nm, β resembles the full width at half maximum (FWHM) in radians and θ indicates the peak positions in radians. Here, d signifies the mean diameter of NPs, λ represents the wavelength of the x-ray radiation source and β shows the angular full width at half maximum of the XRD peak at the specified angle θ. The micro dislocation densities are computed using the subsequent method, such as,

Dislocation Density $\rho = n/D^2$

The size, shape and morphology of CeO2 are investigated using SEM technology and the basic composition of the nanoparticles is determined using the EDAX method. In addition to showing the uniform distribution of silver and CeO2 nanoparticles, the XRD data reveal the creation of silver nanoparticles in cubic and face-centered lattice structures, as well as Silver-doped ceramic oxide nanoscale. The average size of the crystallite for untreated ceramic oxide was 19.27 nm whereas that of Ag-doped ceramic oxide nanoparticles was 18.21 nm.

Various equations are used to determine different parameters. Using a formula and computing the square root of each side, the lattice parameters a, b and c are determined.

1/d2 = (h2+k2+l2)/a2

The optical behavior of the produced nanocomposite was assessed using a UV-visible spectrophotometer which represents the photocatalyst's absorption wavelength. The absorption wavelength of a photocatalyst must be determined in order to calculate the energy difference between incoming light and the photocatalyst's band gap. To excite sufficient electrons, the disparity in energy between photocatalysts' conduction and valence bands needs to be minimized. As a result, the researchers obtained the optical absorption spectrum of the synthesized CeO2.

The current study was similar to a few previous investigations undertaken by other researchers. Kravtsov et al. (2023) revealed that CeO2-Ag nanocomposites, independent of the silver content, demonstrated greater photocatalytic activity than pure nanosized CeO2 [16]. Negi et al. (2019) demonstrated that the results obtained for Ag/CeO2 composites clearly revealed significantly better catalytic and antibacterial characteristics in comparison to pure CeO2 [17]. Murugadoss et al. in 2021 synthesized and characterized pure and Ag/CeO2 nanoparticles using various techniques. The presence of Ag on CeO2 surface was confirmed through XRD, XPS, and EPR spectroscopy. UV absorption peaks of pure and Ag decorated CeO2 was found at 320 nm and 430 nm, respectively. The enhanced catalytic performance of Ag/CeO2 composites depends on the preparation method determining homogeneous morphology and Ag distribution on the ceria surface [18]. Saravanankumar et al. (2016) illustrated that the strong photocatalytic activity of Ag/CeO2 nanocomposites can be related to the surface plasmon resonance effect of Ag nanoparticles that are widely scattered on the surface of CeO2 [19].

The textile, dyeing, and printing industries are major sources of industrial wastewater, which often contains significant amounts of Azo dyes. These dyes are widely used for their vibrant colors and chemical stability but are notorious for their environmental and health hazards. Azo dyes are difficult to degrade and can persist in water bodies, posing risks to aquatic life and human health through bioaccumulation [18]. A recent study by Vedhantham et al. depicted increased photocatalytic efficiency and improved stability and reusability. The green synthesized Ag-doped CeO2/MgAl-LDH nanoclay showed remarkable photocatalytic activity, achieving a 95% degradation efficiency within 30 minutes. Its unique hexagonal plate-like morphology, with a narrow band gap, facilitates efficient generation of reactive species. The composite also showed excellent stability over multiple cycles, making it a promising candidate [20].

Silver-doped cerium oxide (Ag-CeO_2) offers a promising solution for the photocatalytic degradation of Azo dyes under sunlight. This material acts as an efficient photocatalyst, utilizing solar energy to break down the complex molecular structures of Azo dyes into less harmful substances. The doping of silver enhances the photocatalytic properties of cerium oxide by improving charge separation and reducing the recombination rate of photogenerated electron-hole pairs, thereby increasing the overall efficiency of the degradation process. Using Ag-CeO_2 for photocatalytic degradation under sunlight is particularly advantageous because it leverages a free and abundant energy source, sunlight, making the process cost-effective and sustainable. Unlike traditional wastewater treatment methods that may require high energy inputs or the use of harmful chemicals, Ag-CeO_2 provides an eco-friendly alternative. This technology can be integrated into existing industrial wastewater treatment systems, helping industries meet environmental regulations while reducing their environmental footprint [21].

5. Conclusions:

Ceria nanoparticles were successfully prepared by the sol-gel route. Prepared nanocomposites were activated in direct sunlight when the series was performed keeping the basic pH environment (a series of pH 3, 7 and 11 of ceria powder was performed when the pH of all selected dyes was 11). For the pH 11 of all selected dyes (methylene red, methylene blue, methylene orange and malachite green) treated with the ceria powder, we get the highest photocatalytic activity as it was degraded very fast under sunlight directly. More efficient dye was malachite green which degraded quickly as compared to other dyes. Cerium oxide nano

particles were prepared by sol-gel method. These nanoparticles are used for degradation of dye solutions. The SEM results showed that the surface morphology of ceria composite is spherical shape with nonuniform grains of (~8-20 nm) size. XRD results showed that the average crystallite size of pure ceria is 19.29 nm and silver doped cerium oxide is 18.7 nm. Improved optical properties resulted in better photocatalytic performance.

Conflict of interest:

There is no conflict of interest among the authors.

References:

[1] Y. Yang, H. Liao, Z. Tong, and C. Wang, "Porous Ag/polymer composite microspheres for adsorption and catalytic degradation of organic dyes in aqueous solutions," *Composites Science and Technology,* vol. 107, pp. 137-144, 2015.

[2] M.A. Tahir, H.N. Bhatti, and M. Iqbal, "Solar Red and Brittle Blue direct dyes adsorption onto Eucalyptus angophoroides bark: Equilibrium, kinetics and thermodynamic studies," *Journal of Environmental Chemical Engineering,* vol. 4, pp. 2431-2439, 2016.

[3] M. Han, S. Zhu, S. Lu, Y. Song, T. Feng, S. Tao, J. Liu, and B. Yang, "Recent progress on the photocatalysis of carbon dots: Classification, mechanism and applications," *Nano Today,* vol. 19, pp. 201-218, 2018.

[4] N.K. Eswar, V.V. Katkar, P.C. Ramamurthy, and G. Madras, "Novel AgBr/Ag3PO4 decorated ceria nanoflake composites for enhanced photocatalytic activity toward dyes and bacteria under visible light," *Industrial & Engineering Chemistry Research,* vol. 54, pp. 8031-8042, 2015.

[5] M.R. Hoffmann, S.T. Martin, W. Choi, and D.W. Bahnemann, "Environmental applications of semiconductor photocatalysis," *Chemical reviews,* vol. 95, pp. 69-96, 1995.

[6] C. Su, C.-M. Tseng, L.-F. Chen, B.-H. You, B.-C. Hsu, and S.-S. Chen, "Sol–hydrothermal preparation and photocatalysis of titanium dioxide," *Thin Solid Films,* vol. 498, pp. 259-265, 2006.

[7] Y. Wang, Y. Huang, W. Ho, L. Zhang, Z. Zou, and S. Lee, "Biomolecule-controlled hydrothermal synthesis of C–N–S-tridoped TiO2 nanocrystalline photocatalysts for NO removal under simulated solar light irradiation," *Journal of Hazardous materials,* vol. 169, pp. 77-87, 2009.

[8] D.B. Hamal and K.J. Klabunde, "Synthesis, characterization, and visible light activity of new nanoparticle photocatalysts based on silver, carbon, and sulfur-doped TiO2," *Journal of colloid and interface science,* vol. 311, pp. 514-522, 2007.

[9] O.H. Carp, "CL, and Reller, A," *Prog. Solid State Chem,* vol. 32, p. 33, 2004.

[10] K.J. Klabunde, "Visible and UV Light Photocatalysts in Environmental Remediation," in *Nanoscale Materials in Chemistry: Environmental Applications*, ed: ACS Publications, 2010, pp. 179-189.

[11] S. Klosek and D. Raftery, "Visible light driven V-doped TiO2 photocatalyst and its photooxidation of ethanol," *The Journal of Physical Chemistry B,* vol. 105, pp. 2815-2819, 2001.

[12] N. Sobana, M. Muruganadham, and M. Swaminathan, "Nano-Ag particles doped TiO2 for efficient photodegradation of direct azo dyes," *Journal of Molecular Catalysis A: Chemical,* vol. 258, pp. 124-132, 2006.

[13] M. Shafique, M. S. Mahr, M. Yaseen, and H. N. Bhatti, "CQD/TiO2 nanocomposite photocatalyst for efficient visible light-driven purification of wastewater containing methyl orange dye," *Materials Chemistry and Physics,* vol. 278, p. 125583, 2022.

[14] H. Balavi, S. Samadanian-Isfahani, M. Mehrabani-Zeinabad, and M. Edrissi, "Preparation and optimization of CeO2 nanoparticles and its application in photocatalytic degradation of Reactive Orange 16 dye," *Powder technology,* vol. 249, pp. 549-555, 2013.

[15] X. Du and T. E. Graedel, "Global rare earth in-use stocks in NdFeB permanent magnets," *Journal of Industrial Ecology,* vol. 15, pp. 836-843, 2011.

[16] A. A. Kravtsov, A. V. Blinov, A. A. Nagdalian, A. A. Gvozdenko, A. B. Golik, M. A. Pirogov, M. A. Kolodkin, N. S. Alharbi, S. Kadaikunnan, and M. Thiruvengadam, "Acid-Base and Photocatalytic Properties of the CeO2-Ag Nanocomposites," *Micromachines,* vol. 14, p. 694, 2023.

[17] K. Negi, A. Umar, M. Chauhan, and M. S. Akhtar, "Ag/CeO2 nanostructured materials for enhanced

photocatalytic and antibacterial applications," *Ceramics International,* vol. 45, pp. 20509-20517, 2019.

[18] G. Murugadoss, D.D. Kumar, M.R. Kumar, N. Venkatesh, and P. Sakthivel, "Silver decorated CeO2 nanoparticles for rapid photocatalytic degradation of textile rose bengal dye," *Scientific Reports,* vol. 11, p. 1080, 2021.

[19] K. Saravanakumar, M.M. Ramjan, P. Suresh, and V. Muthuraj, "Fabrication of highly efficient visible light driven Ag/CeO2 photocatalyst for degradation of organic pollutants," *Journal of Alloys and Compounds,* vol. 664, pp. 149-160, 2016.

[20] K. Vedhantham, K. Karthik, P. Keerthi & K. Ramalingam, (2025). Biogenic Novel Z-scheme Ag–CeO2/MgAl-LDH composite for enhanced photocatalytic dye degradation. Materials Chemistry and Physics, 337, 130539.

[21] S.B. Madduri, & R.R. Kommalapati. Photocatalytic degradation of azo dyes in aqueous solution using TiO2 doped with rGO/CdS under UV irradiation. Processes, 12(7), 1455, 2024.